Title	Solvent-dependent switch of ligand donor ability and catalytic activity of ruthenium(II) complexes containing pyridinylidene amide (PYA) n-heterocyclic carbene hybrid ligands
Authors(s)	Leigh, Vivienne, Carleton, Daniel J., Olguín, Juan, Müller-Bunz, Helge, Wright, L. James, Albrecht, Martin
Publication date	2014-07-21
Publication information	Leigh, Vivienne, Daniel J. Carleton, Juan Olguín, Helge Müller-Bunz, L. James Wright, and Martin Albrecht. "Solvent-Dependent Switch of Ligand Donor Ability and Catalytic Activity of ruthenium(II) Complexes Containing Pyridinylidene Amide (PYA) N-Heterocyclic Carbene Hybrid Ligands" 53, no. 15 (July 21, 2014).
Publisher	American Chemical Society
Item record/more information	http://hdl.handle.net/10197/6823
Publisher's statement	This document is the unedited author's version of a Submitted Work that was subsequently accepted for publication in Inorganic Chemistry, copyright © American Chemical Society after peer review. To access the final edited and published work, see http://pubs.acs.org/doi/abs/10.1021/ic501026k.
Publisher's version (DOI)	10.1021/ic501026k

Solvent-Dependent Switch of Ligand Donor Ability and Catalytic Activity of Ruthenium(II) Complexes Containing Pyridinylidene Amide (PYA) N-heterocyclic Carbene Hybrid Ligands

Vivienne Leigh,[†] Daniel J. Carleton,[‡] Juan Olguin,[†] Helge Mueller-Bunz,[†] L. James Wright,*[‡] Martin Albrecht*[†]

[†] *School of Chemistry & Chemical Biology, University College Dublin, Belfield, Dublin 4, Ireland*

[‡] *School of Chemical Sciences, University of Auckland, Auckland, New Zealand*

E-mail: martin.albrecht@ucd.ie, lj.wright@auckland.ac.nz

Abstract

Chelating ligands incorporating both *N*-[1-alkylpyridin-4(1H)-ylidene]amide (PYA) and *N*-heterocyclic carbene (NHC) donor sites were prepared and used for the synthesis of ruthenium(II) complexes. Cyclic voltammetry, NMR and UV-vis spectroscopy of the complexes indicate a solvent-dependent contribution of the limiting resonance structures associated with the ligand in solution. The neutral pyridylidene imine structure is more pronounced in apolar solvents (CH_2Cl_2), while the mesoionic pyridinium amide form is predominant in polar solvents (MeOH, DMSO). The distinct electronic properties of these hybrid PYA-NHC ligands in different solvents have a direct influence on the catalytic activity of the ruthenium center, *e.g* in the dehydrogenation of benzyl alcohol to benzaldehyde. The activity in different solvents qualitatively correlates with their permittivity.

Introduction

The development of powerful donor ligands plays a central role in the advancement of homogenous catalysis and in coordination and organometallic chemistry in general.[1] Flexible ligands, specifically ligands which exhibit varying degrees of electron donor ability are of interest for catalytic applications, as they may stabilise different intermediates of the catalytic cycle. In addition, a flexible structure may allow for tuning of electronic parameters about the metal center. Recent advances in these directions include the introduction of remote anionic functionalities as well as cationic ammonium and imminium units that are conjugated with the ligand donor site binding to the metal center, for example complexes **I–IV** (Fig. 1).[2]
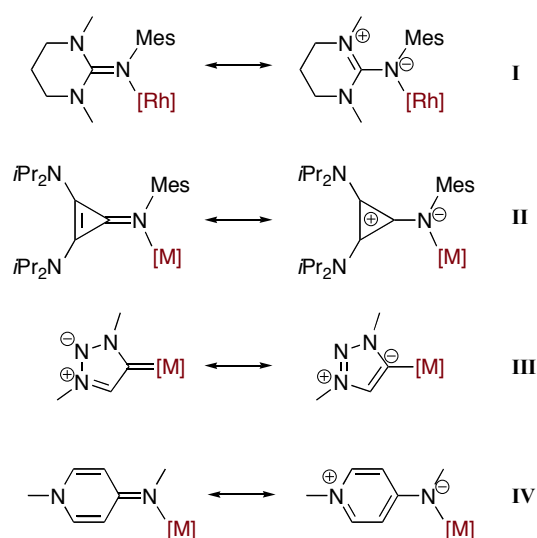

Figure 1 Selected examples of complexes with limiting resonance structures that feature either a formally neutral or a formally anionic donor site.

1H-pyridinylidene amines (PYEs) such as the pyridin-4-ylidene amine **IV** are a particularly attractive subclass of such donor-flexible ligands because their steric and electronic properties are easily modified through facile incorporation of different groups at the pyridyl and amine nitrogen atoms.[3] One related class of ligands involves the incorporation of an acyl substituent at the amine nitrogen, which yields so-called pyridinylidene-amides (PYAs) (Scheme 1).[4,5] The introduction of a carbonyl group adjacent to the donor nitrogen principally enhances the charge-conjugated system and also enhances the coordinative flexibility of the ligand through the availability of resonance forms involving an anionic oxygen unit (Scheme 1). PYEs and PYAs share some common properties with those of NHCs, specifically they were demonstrated to be strong σ donors and have a net overall neutral charge.[5,6] However, DFT studies predict that the nitrogen-metal bond is much more

polarised than the carbon-metal bond in NHC complexes, and hence is more susceptible to nucleophilic and electrophilic attack.[6] This reactivity may explain, at least in some part, the scarce application of PYAs as ligands to transition metals up to now. The first and thus far only complexes involve palladium and rhodium as the metal center,[5] and the palladium complexes show promising activity in Suzuki cross coupling reactions.

Scheme 1 Potential limiting resonance structures of pyridinylidene amides (PYAs).
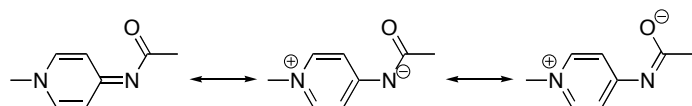
Based on the similar donor properties of PYAs and NHCs, the preparation of complexes that incorporate both ligand classes may be of interest. In contrast to PYAs, NHCs have been extensively studied in catalytic applications.[7] They are of benefit in catalysis as they often bind tightly to metal centers and thus prevent metal dissociation and catalyst degradation.[8] In addition, a PYA-NHC hybrid system affords a neutral bidentate ligand that has two dissimilar strong σ-donors, comprised of a relatively soft carbon donor from the NHC site with significant covalent bonding preference, while the other is a harder nitrogen donor that favors ionic interactions. Such different properties may indeed be beneficial for catalytic applications.

Density Functional Theory (DFT) calculations and single-crystal X-ray analysis have been used previously to determine the most predominant resonance stucture contributions of PYE and PYA complexes in the solid state.[3,5,6] However, to the best of our knowledge the structure that these complexes adopt in solution has never been fully explored. Herein we describe a set of ruthenium complexes where the predominant resonance structure of the ligand can be controlled by the nature of the solvent, thus leading to a responsive ligand system with potential for catalytic applications.

Results and Discussion

Synthesis. The NHC-PYA ligand precursor was prepared by reacting 4-aminopyridine with bromoacetylbromide in the presence of a base to form 2-bromo-N-(4-pyridyl) acetamide **1** as reported previously (Scheme 2).[11,12] Acylation was also successfully performed with chloroacetylchloride,[13] however subsequent steps were less clean and much lower yielding than when using the bromo analogue. Substitution of the bromide with an *N*-alkylated

imidazole in CH$_3$CN yielded the corresponding imidazolium salt intermediates which were not purified.[14] A ^{1}H NMR spectroscopic analysis of the crude imidazolium salts showed the expected large downfield shift of the NC*H*N proton from ca. 7.7 ppm in the imidazole to 8.91 ppm and 9.12 ppm in the azolium salts containing a Me and *i*Pr wingtip group, respectively. The bridging CH$_2$ singlet also shifted considerably from 4.02 ppm in **1** to 4.2 ppm upon imidazolium salt formation.

Scheme 2 Synthesis of NHC complexes **3a** and **3b**.
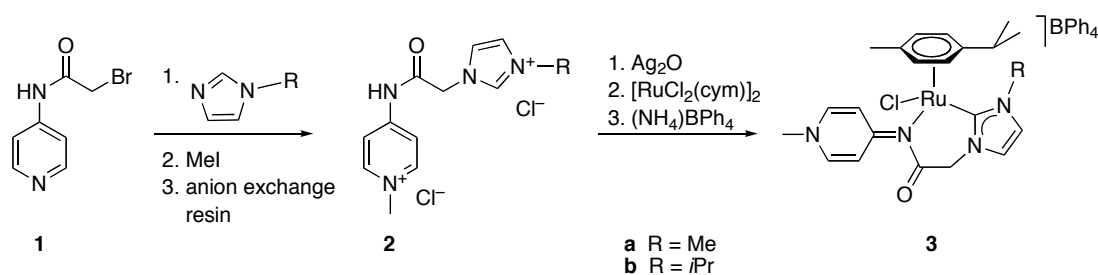
The imidazolium salts were treated directly with iodomethane in DMSO to give the mixed anion salt. The NC*H*N proton undergoes a marginal downfield shift to 9.00 ppm and 9.18 ppm in **a** and **b**, respectively. The mixed anion salt was then passed through an ion exchange column to exchange the mixed anions to chlorides. This alteration also prevents mixed anions in the subsequently formed complex. Formation of the products **2a** and **2b** was confirmed in the ^{1}H NMR spectra by the substantial shift of the pyridine ring doublets upon alkylation. For example, the α protons are observed at 8.42 ppm in the monocationic salt and are shifted downfield to 8.75 ppm in **2a** and 8.77 ppm in **2b** upon pyridine alkylation. The second doublet moves from 7.65 ppm to 8.03 ppm in **2a** and 8.01 ppm in **2b**. The bridging CH$_2$ singlet is also significantly deshielded and moves from 4.2 ppm to 5.3 ppm upon methylation. A slight shift of the NC*H*N proton lower field to 9.08 ppm in **2a** and 9.26 ppm in **2b** was noted in the ^{1}H NMR spectra. The carbonyl group displayed a characteristic absorption at ν = 1794 cm^{-1} and ν = 1795 cm^{-1} for **2a** and **2b**, respectively, in the IR spectra.

The pyridinylidene-amide ruthenium complexes **3a** and **3b** were prepared in 50% and 37% yield, respectively, via transmetalation of the corresponding silver intermediate by reacting the salts **2a** or **2b** in a one-pot synthesis with Ag$_2$O and [RuCl$_2$(*p*-cymene)]$_2$ in CH$_3$CN. One equivalent of Ag$_2$O was added to both coordinate the carbene and also deprotonate the N*H*. When only half an equivalent of Ag$_2$O was added no carbene complexation was observed and the acidic proton at about 9 ppm was still visible in the ^{1}H NMR spectra. Therefore, the silver oxide deprotonates the amide before deprotonating the

imidazolium salt, which is not surprising as the amide[15] has a pK$_a$ of about 15 compared to about 20 for the imidazolium entity.[16] For solubility purposes the non-coordinating anion was exchanged for [BPh$_4$]$^-$. Complexes **3a** and **3b** were highly air and water stable and anhydrous or inert conditions were not necessary for the synthesis and purification. The complexes are racemic, however no attempts were made to resolve enantiomers.

NMR, mass spectrometry and elemental analysis confirmed the formation of the complexes. The most diagnostic feature in the ^{1}H NMR spectra was the loss of the acidic proton in the C2 position of the imidazolium salts, suggesting carbene coordination. In addition, the methyl groups of the isopropyl wingtip in complex **3b** are diastereotopic and appear as two doublets at 1.09 and 0.94 ppm as compared with one single doublet at 1.5 ppm in **2b**. Similarly, the methyl wingtip in **2a** also shifted upfield from 3.94 ppm to 3.84 ppm upon complexation. Bidentate ligand coordination was indicated by the emergence of an AB doublet between 4 and 5 ppm for the bridging CH$_2$ group ($^2J_{HH}$ = 13.4 H*z*), suggesting a pseudo axial/equatorial arrangement of these two diastereotopic protons. This split, along with the disappearance of the N*H* proton at about 11 ppm suggests that the amide nitrogen is also coordinated to the ruthenium metal center and forms a chelate. The *N*-bound CH$_3$ of the pyridine has a significant shift upfield from 4.19 ppm and 4.20 ppm in **2a** and **2b** to 4.04 ppm and 4.01 ppm in **3a** and **3b**, respectively. The carbene carbon appears at 172.4 ppm in complex **3a** and at 171.4 ppm in complex **3b** in the ^{13}C NMR spectra which is in good agreement with related carbene ruthenium complexes.[17] The carbonyl carbon is only moderately affected by the amide coordination and is slightly deshielded from 167 ppm in **2** to 173.3 ppm and 173.9 ppm in **3a** and **3b** respectively.

Interestingly, when the ^{1}H NMR analyses were run in CD$_2$Cl$_2$ rather than DMSO significant differences were observed for the shifts of the two pyridine doublets while most other frequencies remained essentially unaffected. For example in **2a** the two doublets appear at 8.06 ppm and 8.25 ppm (Δδ = 0.19 ppm), whereas in DMSO, the difference is larger (δ$_H$ 8.02 ppm and 8.35 ppm (Δδ = 0.33 ppm). The ^{1}H NMR spectrum measured in MeOD revealed a similar difference to that recorded in DMSO. The larger shielding difference in DMSO and MeOH compared to the resonance frequencies in CD$_2$Cl$_2$ suggests a predominance of resonance structure **B** in polar solvents (Scheme 3). In such a structure, the α protons are in close vicinity of the positively charged nitrogen atom and hence relatively deshielded. In CD$_2$Cl$_2$, on the other hand both doublets are in magnetically more similar environments, which suggests an increased relevance of resonance structure **A**. Very similar spectral changes were noted in a related metal-free system of PYE-type pyridoneimines upon

variation of the polarity of solvents.[18] In the absence of nitrogen coordination to the metal center, the predominance of the neutral resonance structure **A** was supported in those studies by the asymmetry of the heterocyclic protons due to the exocyclic C=N double bond and consequentially a hindered rotation about this bond.

Scheme 3 Limiting resonance structures **A** and **B** of complex **3**.
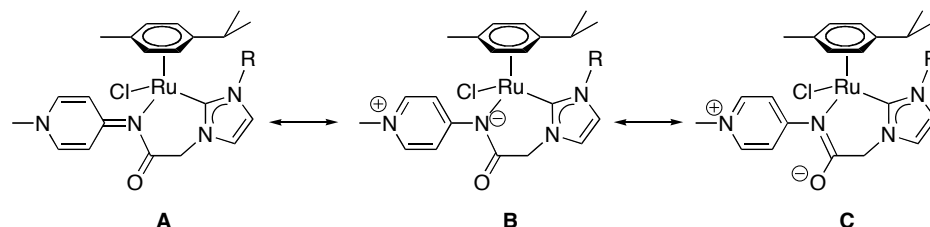
The formation of **3b** was unambiguously confirmed by single crystal X-ray diffraction analysis. Suitable crystals of this complex were obtained by diffusion of Et$_2$O into a CHCl$_3$ solution of **3b**. The molecular structure features the classical three-legged piano-stool geometry with the ruthenium center in a pseudo-tetrahedral geometry. The Ru–C1 bond length is 2.036(2) Å, which is typical of these ruthenium piano-stool complexes.[19] In the pyridyl heterocycle, C9–C10 (1.419(3) Å) and C9–C13 (1.408(3) Å) are significantly longer than C11–C10 (1.365(3) Å) and C12–C13 (1.370(3) Å), indicating predominance of the neutral resonance structure **A** in the solid state with less contribution from a delocalised aromatic system **B** or **C** (Scheme 3).[20] The angle of the pyridine centroid–N4–C14 is 179° and the sum of the angles around the pyridine nitrogen (N4) is 359.99(20)° as may be expected for a sp^2-hybridised nitrogen center.[21] These conclusions are in agreement with previous studies on related PYE compounds by Douthwaite and co-workers,[3a] which indicated a predominantly aminopyridinium-like structure **B** in the solid state, with some double bond character in the heterocycle.
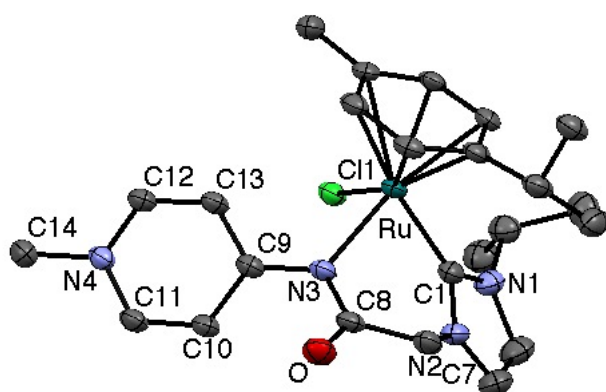
Figure 2 ORTEP representation of complex **3b** (50% probability level). Hydrogen atoms, co-crystallised CHCl$_3$ molecule, and the non-coordinated BPh$_4^-$ anion was omitted for clarity.

Table 1 Selected bond lengths (Å) and angles (°) in complex **3b**

Ru1–C1	2.036(2)	C1–Ru1–N3	83.30(8)
Ru1–N3	2.168(17)	C1–Ru1–Cl1	85.80(7)
Ru–Cl1	2.4028(5)	N3–Ru1–Cl1	87.70(5)
C9–C13	1.408(3)	C13–C9–C10	114.9(2)
C9–C10	1.419(3)	C12–N4–C11	119.01(19)
C13–C12	1.370(3)	C14–N4–C11	120.25(18)
C10–C11	1.365(3)	C14–N4–C12	120.73(19)
C12–N4	1.349(3)		
C11–N4	1.351(3)		
N4–C14	1.476(3)		
N3–C9	1.377(3)		

Spectroscopic and Electrochemical properties. To investigate further the solvent-dependence of the structure of these complexes, electrochemical measurements were carried out. In CH$_2$Cl$_2$ cyclic voltammetry (CV) experiments revealed an irreversible, presumably metal-centered, oxidation at E_{pa} = +0.91 V vs SCE for **3a** and +0.90 V for **3b** (Figure S1). However, when the measurement was performed in MeOH, significantly lower oxidation potentials of E_{pa} = +0.79 V for **3a** and +0.75 V for **3b** were obtained (Figure S2). These differences are quite substantial considering ferrocene has an $E_{1/2}$ of +0.46 V in CH$_2$Cl$_2$ and +0.52 V in MeOH,[22] which is a difference of 60 mV compared with 120 and 150 mV measured for complexes **3a** and **3b**. These differences are therefore too large to be accounted for merely by solvent effects and indicate that changes in the ligand donor strengths are involved. Easier oxidation of the ruthenium center in MeOH suggests a stronger ligand

8

donation in this solvent. Such an effect is likely imparted by the mesoionic resonance form **B** in Scheme 3. The neutral resonance form **A** features a neutral π-acidic imine donor rather than an anionic amide NR_2^-, and this form would be expected to be more relevant in less polar CH_2Cl_2. This conclusion is in agreement with the higher oxidation potential and the relative assignment based on NMR spectroscopy (see above). CV measurements on complex **4** (Figure 3), which contains a neutral imine-like pyridine donor in place of the PYA donor, show an irreversible oxidation potential at +0.90 V (CH_3CN vs SCE).[23] This is highly reminiscent of the oxidation potential of **3a/b** in CH_2Cl_2 but significantly higher than **3a/b** in polar solvents. The lower oxidation potentials observed for **3a/b** in polar solvents are consistent with the PYA ligands behaving as stronger σ-donors with larger relative contributions of mesoionic resonance form **B** (Scheme 3) in solvents of this type.

Table 2 Spectroscopic and electrochemical data of **3a** and **3b**

complex	E_{pa} (V)[a]		λ_{1000} (nm)[b]	
	MeOH	CH_2Cl_2	MeOH	CH_2Cl_2
3a	+0.79 V	+0.91 V	208 nm	235 nm
3b	+0.75 V	+0.90 V	210 nm	240 nm

[a] Sweep rate 400 mV s^{-1}, potentials *vs* SCE referenced to Fc$^+$/Fc, $E_{1/2}$ = +0.46 V (CH_2Cl_2), +0.52 V (MeOH)
[b] λ_{1000} is the wavlength at which ε = 1000 M^{-1} cm^{-1}
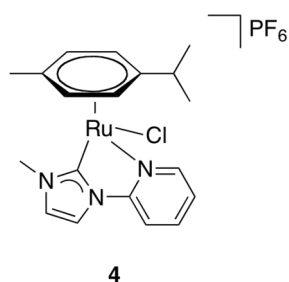

4

Figure 3 Pyridyl-functionalised NHC ruthenium complex **4** (ref 23), an analogue of complex **3**.

UV-Vis spectroscopy corroborates this trend. Figure 4 shows the UV-vis spectrum of **3a** measured in mixtures of MeOH and CH_2Cl_2 at various ratios. Complex **3a** displays a strong absorption below around 240 nm and a very weak and broad absorption band with a λ_{max} of 275 nm. The band at lower energy is not solvent dependent, whereas the band evolving around 240 nm shows a distinct solvent-dependence onset (Figure 4). The absorption becomes more red-shifted as the solvent becomes less polar. This shift is illustrated by considering the wavelength at which the arbitrarily chosen threshold ε = 1,000 M^{-1} cm^{-1} is reached. In 100% MeOH, this value is achieved at 208 nm while in 100% CH_2Cl_2

solution, the extinction coefficient reaches this height already at 235 nm. Interestingly, the shift is non-linear and as little as 1% CH_2Cl_2 in MeOH solution shifts the absorption at ε = 1,000 M^{-1} cm^{-1} from 208 nm to 221 nm (inset Figure 4). The shift then becomes gradual upon further increasing the CH_2Cl_2 ratio. These electronic changes corroborate the previous observations from NMR and electrochemical analyses and suggests a solvent-dependent flexibility of the ligand π-system and a tunable donor ability of the amide ligand through limiting resonance structures **A** and **B** that strongly depend on solvent polarity.[18,24]
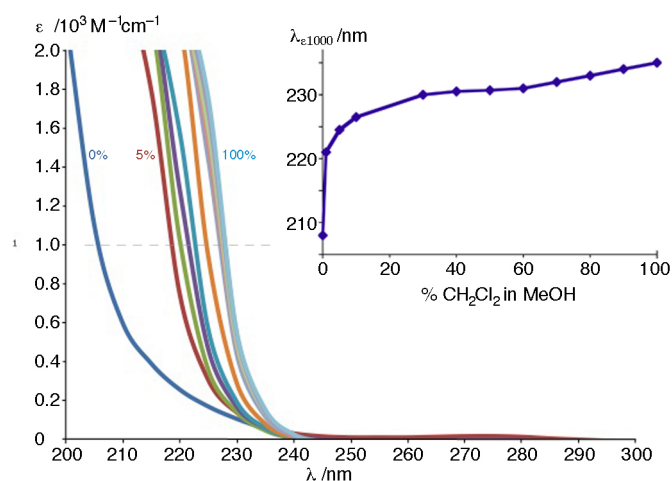

Figure 4 UV-vis spectra of **3a** in different MeOH/CH_2Cl_2 solvent ratios (% refers to CH_2Cl_2 fraction); inset shows the redshift of the wavelength at which ε = 1000 M^{-1} cm^{-1} ($\lambda_{\varepsilon 1000}$) upon increasing the fraction of CH_2Cl_2 in MeOH.

Infrared spectroscopy of **3a** revealed a strong amide absorption at 1606 cm^{-1} in CH_2Cl_2 and 1605 cm^{-1} in MeOH. Bands in this region are predominantly associated with the stretching frequency of the amide I band. Since these values are virtually identical this suggests that the carbonyl unit is essentially unaffected by solvent changes. Accordingly, resonance structures such as **C** are probably of minor relevance (Scheme 3). Presumably the ionic character of the N–Ru bond in resonance structure **B** disfavors migration of the negative charge to more remote positions.

Catalysis. Complex **3a** was tested in the dehydrogenation of benzyl alcohol to benzaldehyde.[25] Catalytic reactions were carried out in solvents of varying dielectric constants (ε_r) to exploit the solvent-dependent properties of the ruthenium center. When the catalysis was performed in 1,4-dioxane or toluene, which have similarly low permittivity (ε_r = 2.25 and 2.38, respectively),[26] no conversion was observed after 2 h (Table 3). In dichlorobenzene a very moderate conversion of 6% was obtained (ε_r = 9.93), while conversion rose to 32% in

DMSO ($\varepsilon_r = 46.67$). This higher activity was attributed to an increased relevance of resonance structure **B** over **A** upon increasing the permittivity which presumably increases the donor strength of the NHC-PYA ligand (*cf.* electrochemistry section). Strongly donating ligands are important in this oxidation process for labilizing the chloride ligand, which enables substrate coordination.[27] Moreover, solvents with a high dielectric constant solubilize the dissociated chloride ligand better and are therefore expected to shift the equilibrium further towards the ion-separated species. It is worth emphasizing that the donor flexibility of the NHC-PYA ligand has a distinct impact. Significantly, when using the pyridyl-substituted NHC ruthenium complex **4**, in which a swap between mesoionic and neutral resonance forms of the N-donor ligand is supressed, the reactivity profile is different and does not correlate with the dielectric constant. Accordingly, the activity of complex **3a** is not a mere effect of chloride stabilization but directly affected by the PYA and its flexible donor properties.

Table 3. Catalytic dehydrogenation of benzyl alcohol to benzaldehyde[a)]
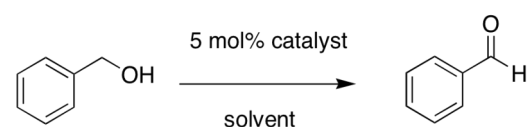
	3a	**4**	Dielectric constant (ε_r)
1,4-dioxane	1%	7%	2.25
toluene	0%	6%	2.38
1,2-dichlorobenzene	6%	25%	9.93
DMSO	32%	6%	46.7

[a)] General reaction conditions: benzyl alcohol (0.2 mmol), Cs_2CO_3 (0.04 mmol), anisole (internal standard, 0.2 mmol) and complex **3a** or **4** (0.01 mmol, 5 mol%) in the corresponding solvent (2.0 mL) at 110°C, NMR spectroscopic yields after 2 h; dielectric constants from ref. 25.

The complexes were also tested in the transfer hydrogenation of benzophenone to diphenylmethanol in *iso*-propanol. Moderate conversions of up to 20% for **3a** and **3b** after 6 h at reflux were obtained. No further conversions after 24 h were observed. However, black particles were detected and this is presumably due to decomposition of the complex under these conditions.

Conclusions

A set of novel complexes with ligands that contain both PYA and NHC donors have been prepared and fully characterised. Electrochemical measurements, NMR and UV-vis spectroscopic analyses strongly suggest a solvent-dependent resonance structure of the ligand

framework, with a neutral structure predominating in apolar solvents while in polar media there is a larger contribution from a mesoionic structure featuring an anionic amidate donor site at ruthenium. UV-vis spectroscopy showed that with as little as 1% CH_2Cl_2 in a methanol solution, the neutral resonance structure gains substantially in relevance. Hence PYA-type ligands have a flexible donor strength, which is triggered by the solvent and presumably also by the central metal atom. Such dynamic donor properties paired with the synthetic flexibility of these NHC-PYA hybrid ligands may therefore find application with a variety of metals in catalytic redox processes.

Experimental section

General. 2-bromo-N-(4-pyridyl) acetamide **1** and *N*-isopropyl imidazole were prepared via reported procedures.[11,28] All other starting materials and reagents were obtained from commercial sources and used as received unless otherwise stated. NMR spectra were recorded on Varian spectrometers operating at 400 or 500 MHz. Chemical shifts are reported in δ (ppm) relative to internal Me_4Si in $CDCl_3$ or residual protio solvents. ^{13}C NMR resonances were assigned with the aid of two-dimensional cross-coupling experiments. UV-vis spectra were recorded with a Varian 50 Spectrometer. IR spectra were obtained on a FTIR spectrometer, and are reported here in units of cm^{-1}. Elemental analysis was performed on an Exeter Analytical CE440 elemental analyzer. High-resolution mass spectrometry was carried out with a Micromass/Waters Corp. USA liquid chromatography time-of-flight spectrometer equipped with an electrospray source.

General procedure for the synthesis of imidazole-substituted pyridinium amides. The substituted imidazole (5 mmol) and 2-bromo-N-(4-pyridyl) acetamide **1** (0.64 g, 3 mmol) were refluxed in CH_3CN (20 mL) for 12 h. After cooling to room temperature, the solvent was removed and the solid was re-dissolved in MeOH (2 mL) and precipitated from Et_2O (15 mL). The crude salt was dried, dissolved in DMSO (5 mL) and iodomethane (0.3 mL, 5mmol) was added. The solution was stirred at 60 °C for 12 hours. After repeated precipitation from MeOH (2 mL) and Et_2O (15 mL) the residue was re-dissolved in MeOH (20 mL) and passed through a Dowex ion-exchange column. The solvent was removed in vacuo to give the pure product.

Synthesis of 2a. Compound **2a** was prepared via the general procedure using 1-methylimidazole (0.41 g, 5 mmol) and was obtained as a yellow solid (0.50 g, 55% yield). [1]H

NMR (DMSO–D$_6$, 500 MHz): δ = 11.89 (bs, 1H, NH), 9.08 (s, 1H, NCHN), 8.75 (d, 2H, $^3J_{HH}$ = 7.2 Hz, H$_{pyr}$), 8.03 (d, 2H, $^3J_{HH}$ = 7.2 Hz, H$_{pyr}$), 7.76 (d, 1H, $^3J_{HH}$ = 1.7 Hz, H$_{imid}$), 7.73 (d, 1H, $^3J_{HH}$ = 1.7 Hz, H$_{imid}$), 5.37 (s, 2H, CH$_2$), 4.19 (s, 3H, CH$_{3\text{-pyr}}$), 3.94 (s, 3H, CH$_{3\text{-imid}}$). ^{13}C{H} NMR (DMSO–D$_6$, 125 MHz): δ = 167.1 (C=O), 147.8 (C$_{pyr}$), 146.9 (CH$_{pyr}$), 138.5 (NCHN), 124.4 (CH$_{imid}$), 123.7 (CH$_{imid}$), 115.3 (CH$_{pyr}$), 52.4 (CH$_2$), 47.1 (CH$_3$), 36.4 (CH$_3$). HR–MS (m/z): 231.1245, calculated for [M–2Cl + H] 231.1251. υ = 1794 cm^{-1}.

Synthesis of 2b. Compound **2b** was prepared via the general procedure using 1-isopropylimidazole (0.55 g, 5 mmol) and was obtained as a yellow solid (0.62 g, 62%). ^{1}H NMR (DMSO–D$_6$, 500 MHz): δ = 11.91 (bs, 1H, NH), 9.26 (s, 1H, NCHN), 8.77 (d, 2H, $^3J_{HH}$ = 7.2 Hz, H$_{pyr}$), 8.01 (d, 2H, $^3J_{HH}$ = 7.2 Hz, H$_{pyr}$), 7.97 (d, 1H, $^3J_{HH}$ = 1.9 Hz, H$_{imid}$), 7.79 (d, 1H, $^3J_{HH}$ = 1.9 Hz, H$_{imid}$), 5.38 (s, 2H, CH$_2$), 4.75 (septet, 1H, $^3J_{HH}$ = 6.7 Hz, CH$_{iPr}$), 4.20 (s, 3H, CH$_{3\text{-pyr}}$), 1.50 (d, 6H, $^3J_{HH}$ = 6.7 Hz, CH$_{3\ iPr}$). ^{13}C{H} NMR (DMSO–D$_6$, 125 MHz): δ = 167.0 (C=O), 151.0 (C$_{pyr}$), 146.8 (CH$_{pyr}$), 136.6 (NCHN), 124.6 (CH$_{imid}$), 120.5 (CH$_{imid}$), 115.3 (CH$_{pyr}$), 52.8 (CH$_{iPr}$), 52.2 (CH$_2$), 47.0 (CH$_3$), 22.7 (CH$_{3\ iPr}$). HR–MS (m/z): 259.1558, calculated for [M–2Cl and H]$^+$ 259.1564. υ = 1795 cm^{-1}.

General procedure for the synthesis of ruthenium *p*-cymene complexes. The pyridinium imidazolium salt **2** (0.33 mmol), Ag$_2$O (0.07 g, 0.33 mmol) and [RuCl$_2$(*p*-cymene)]$_2$ (0.09 g, 0.16 mmol) were dissolved in CH$_3$CN (10 mL) and stirred at 60 $^\circ$C in the absence of light for 12 hours. The suspension was cooled to room temperature and filtered through a pad of Celite. The solvent was removed under reduced pressure. The formed yellow solid was dissolved in MeOH (2 mL) and precipitated from Et$_2$O (15 mL). A saturated aqueous solution of NH$_4$BPh$_4$ (10 mL) was then added to the yellow powder and the product was extracted with CH$_2$Cl$_2$ (3 × 50 mL). The organic layers were combined, dried over MgSO$_4$, filtered and evaporated under reduced pressure to give the pure complex.

Synthesis of 3a. According to the general procedure from **2a** (0.09 g, 0.33 mmol) as a yellow powder (150 mg, 50%). Microanalytically pure crystals were grown from slow diffusion of Et$_2$O into a CHCl$_3$ solution of **3a**. ^{1}H NMR (DMSO–D$_6$, 500 MHz): δ = 8.35 (d, 2H, $^3J_{HH}$ = 7.3 Hz, CH$_{pyr}$), 8.02 (d, 2H, $^3J_{HH}$ = 7.3 Hz, CH$_{pyr}$), 7.54 (d, 1H, $^3J_{HH}$ = 1.9 Hz, CH$_{imid}$), 7.50 (d, 2H, $^3J_{HH}$ = 1.9 Hz, CH$_{imid}$), 7.21–7.15 (m, 8H, H$_{BPh4}$), 6.92 (t, 8H, $^3J_{HH}$ = 9.1 Hz, CH$_{BPh4}$), 6.78 (d, 4H, $^3J_{HH}$ = 9.1 Hz, CH$_{BPh4}$), 5.72–5.68 (m, 3H, H$_{cym}$), 5.55 (d, 1H, $^3J_{HH}$ = 5.7 Hz, CH$_{cym}$), 4.73, 4.67 (2 × d, 1H, $^2J_{HH}$ = 13.4 Hz, CH$_2$), 4.04 (s, 3H, CH$_{3\ pyr}$), 3.84 (s, 3H, CH$_{3\ imid}$), 3.39

(septet, 1H, $^3J_{HH}$ = 6.9 Hz, CH$_{cym}$), 2.04 (s, 3H, CH$_{3\ cym}$), 1.11, 0.97 (2 × d, 6H, $^3J_{HH}$ = 6.9 Hz, CHCH$_3$). ^{13}C{H} NMR (DMSO–D$_6$, 125 MHz): δ = 173.3 (C=O), 172.4 (C–Ru), 163.7, 163.3, 162.9, 162.5 (C$_{BPh4}$), 142.1 (CH$_{pyr}$), 135.3 (CH$_{BPh4}$), 125.1, 125.0 (CH$_{BPh4}$, CH$_{pyr}$, 2 × CH$_{imid}$), 121.9(C=O), 121.2 (CH$_{BPh4}$), 106.7 (C$_{cym}$), 99.9 (C$_{cym}$), 89.9, 84.3, 83.3, 82.9 (CH$_{cym}$), 54.2 (CH$_2$), 45.01 (CH$_{3\ pyr}$), 37.0 (CH$_{3\ imid}$), 30.5 (CH$_{cym}$), 23.0, 21.1 (2 × CHCH$_3$ $_{cym}$), 17.49 (CH$_{3\ cym}$). Elemental analysis for C$_{46}$H$_{48}$BClN$_4$ORu (820.23) × 0.75 CHCl$_3$ calcd: C 61.72, H 5.40, N 6.16; found: C 61.44, H 5.45, N 6.29. HR–MS (m/z): 501.1016, calculated for [M–BPh$_4$]$^+$ 501.0995. υ = 1606 cm^{-1} in CH$_2$Cl$_2$ and 1605 cm^{-1} in MeOH.

Synthesis of 3b. According to the general procedure from **2b** (0.10 g, 0.33 mmol) as a yellow powder (100 mg, 37%). Microanalytically pure sample was obtained from slow diffusion of Et$_2$O into a CH$_3$OH solution of **3b**. Single crystals suitable for X-ray diffraction were grown from slow diffusion of ether into a solution of **3b** in chloroform. ^{1}H NMR (DMSO–D$_6$, 400 MHz): δ = 8.30 (d, 2H, $^3J_{HH}$ = 7.3 Hz, CH$_{pyr}$), 7.96 (d, 2H, $^3J_{HH}$ = 7.3 Hz, CH$_{pyr}$), 7.66 (d, 1H, $^3J_{HH}$ = 2.0 Hz, CH$_{imid}$), 7.55 (d, 2H, $^3J_{HH}$ = 2.0 Hz, CH$_{imid}$), 7.12–7.15 (m, 8H, H$_{BPh4}$), 6.89 (t, 8H, $^3J_{HH}$ = 7.3 Hz, CH$_{BPh4}$), 6.77 (t, 4H, $^3J_{HH}$ = 7.3 Hz, CH$_{BPh4}$), 5.64–5.67 (m, 2H, H$_{cym}$), 5.63 (d, 1H, $^3J_{HH}$ = 5.7 Hz, CH$_{cym}$), 4.70 (septet, 1H, $^3J_{HH}$ = 6.5 Hz, CH$_{iPr}$), 4.72, 4.65 (2 × d, 1H, $^2J_{HH}$ =13.4 Hz, CH$_2$), 4.01 (s, 3H, CH$_{3\ pyr}$), 3.39 (septet, 1H, $^3J_{HH}$ = 6.8 Hz, CH$_{cym}$), 2.00 (s, 3H, CH$_{3\ cym}$), 1.50, 1.29 (2 × d, 6H, $^3J_{HH}$ = 6.5 Hz, CHC$H_{3\ iPr}$) 1.09, 0.94 (2 × d, 6H, $^3J_{HH}$ = 6.8 Hz, CHC$H_{3\ cym}$). ^{13}C{H} NMR (DMSO–D$_6$, 100 MHz): δ = 173.9 (C=O), 171.4 (C–Ru), 166.1, 163.9, 163.6, 163.0 (C$_{BPh4}$), 142.2 (CH$_{pyr}$), 135.5 (CH$_{BPh4}$), 125.3, 125.2 (CH$_{BPh4}$, CH$_{pyr}$, 2 × CH$_{imid}$), 119.2 (CH$_{BPh4}$), 106.5 (C$_{cym}$), 100.5 (C$_{cym}$), 86.3, 84.9, 84.1, 83.7 (CH$_{cym}$), 54.9 (CH$_2$), 51.6 (CH), 45.4 (CH$_{3\ pyr}$), 31.0 (CH$_{cym}$), 24.0, 23.8 (2 × CHCH$_3$ $_{iPr}$), 23.3, 21.6 (2 × CHCH$_3$ $_{cym}$), 17.9 (CH$_{3\ cym}$). Elemental analysis for C$_{48}$H$_{52}$BClN$_4$ORu (847.29) × 1 CH$_3$OH calcd: C 66.85, H 6.41, N 5.85; found: C 67.08, H 5.95, N 5.83. HR–MS (m/z): 529.1312, calculated for [M–BPh$_4$]$^+$ 529.1308. υ = 1606 cm^{-1} in CH$_2$Cl$_2$ and 1606 cm^{-1} in MeOH.

Electrochemistry. Electrochemical measurements were carried out using an EG&G Princeton Applied Research potentiostat model 273A typically at 100 mV s^{-1} sweep rate employing a gastight three-electrode cell under an argon atmosphere. A Pt disk with a 3.80 mm^2 surface area was used as the working electrode and was polished before each measurement. The reference electrode was an Ag/AgCl electrode; the counter electrode was a Pt wire. Bu$_4$NPF$_6$ (0.1 M) in dry CH$_2$Cl$_2$ or MeOH was used as a base electrolyte with analyte

concentrations of approximately 10^{-3} M. The ferrocenium/ferrocene redox couple was used as an internal reference ($E_{1/2} = 0.46$ V vs. SCE).[21]

Catalytic procedures. Typical procedure for oxidation of benzyl alcohol: The catalyst (0.01 mmol), anisole (internal standard, 20 μL, 0.2 mmol), Cs_2CO_3 (13 mg, 0.04 mmol), benzyl alcohol (19 μL, 0.2 mmol) and solvent (2 mL) were placed in a sealed vial and heated to 110 °C. An aliquot (0.1 mL) was taken after 2 h, with $CDCl_3$ (0.6 mL) and analysed by ^{1}H NMR spectroscopy.

Typical procedure for the transfer hydrogenation of benzophenone: The catalyst (0.05 mmol) was weighed directly into the reaction flask. It was stirred, together with KOH (0.05 mL of 2 M soution in H_2O, 0.1 mmol) and iPrOH (5mL) at reflux for 10 min. Then benzophenone (182 mg, 1.0 mmol) was added. Aliquots (0.2 mL) were taken after fixed times, quenched with hexane (2mL), filtered through a short pad of silica and the silica washed with diethyl ether. The combined organic filtrates were evaporated and analysed by ^{1}H NMR spectroscopy.

Crystallographic details. Crystal data for **3b** were collected using an Agilent Technologies SuperNova A diffractometer fitted with an Atlas detector and using monochromated Mo–K_α radiation (0.71073 Å). A complete dataset was collected, assuming that the Friedel pairs are not equivalent. An analytical numeric absorption correction was performed.[29] The structure was solved by direct methods using SHELXS–97[30] and refined by full matrix least-squares on F^2 for all data using SHELXL–97.[30] Hydrogen atoms were added at calculated positions and refined using a riding model. Their isotropic thermal displacement parameters were fixed to 1.2 times (1.5 times for methyl groups) the equivalent one of the parent atom. Anisotropic thermal displacement parameters were used for all non-hydrogen atoms. Disordered solvent was treated with the SQUEEZE procedure as implemented in PLATON.[31] Further crystallographic details are compiled in Table S1. Crystallographic data (excluding structure factors) for **3b** have been deposited with the Cambridge Crystallographic Data Centre as supplementary publication no. CCDC 999483.

Supporting Information Available: Cyclovoltammetry plots and crystallographic data in CIF format.

References

(1)   (a) Engle, K. M.; Yu, J.-Q. *J. Org. Chem.* **2013**, *78*, 8927–8955. (b) The design of ligand systems for immobilisation in novel reaction media, in phosphorus (III) ligands in homogenous catalysis: design and synthesis; Webb, P. B.; Cole Hamilton, D. J., Ed. Wiley and sons: UK, **2012**. (c) Fey, N.; Orpen, A. G.; Harvey, J. N. *Coord. Chem. Rev.* **2009**, *253*, 704–722. (d) Gorin, D. J.; Sherry, B. D.; Toste, F. D. *Chem. Rev.* **2008**, *108*, 3351–3378.

(2)   (a) Bruns, H.; Patil, M.; Carreras, J.; Vazquez, A.; Thiel, W.; Goddard, R.; Alcarazo, M. *Angew. Chem. Int. Ed.* **2010**, *49*, 3680–3683. (b) Cauzzi, D.; Delferro, M.; Graiff, C.; Pattacini, R.; Predieri, G.; Tiripicchio, A. *Coord. Chem. Rev.* **2010**, *254*, 753–764. (c) Thatcher, R. J.; Johnson, D. G.; Slattery, J. M.; Douthwaite, R. E. *Chem. Eur. J.* **2012**, *18*, 4329–4336. (d) Cesar, V.: Lugan, N.: Lavigne, G. *J. Am. Chem. Soc.* **2008**, *130*, 11286–11287. (e) Mathew, P.; Neels, A.; Albrecht, M. *J. Am. Chem. Soc.* **2008**, *130*, 13534–13535. (f) Biju, A. T.; Hirano, K.; Fröhlich, R.; Glorius, F. *Chem. Asian J.* **2009**, *4*, 1786–1789. (g) Tulchinsky, Y.; Iron, M. A.; Botoshansky, M.; Gandelman, M. *Nature Chem.* **2011**, *3*, 525–531. (h) Kolychev, E. L.; Kronig, S.; Brandhorst, K.; Freytag, M.; Jones, P. G.; Tamm, M. *J. Am. Chem. Soc.* **2013**, *135*, 12448–12459. (i) Donnelly, K. F.; Petronilho, A.; Albrecht, M. *Chem. Commun.* **2013**, *49*, 1145–1159.

(3)   (a) Shi, Q.; Thatcher, R. J.; Slattery, J.; Sauari, P. S.; Whitwood, A. C.; McGowan, P. C.; Douthwaite, R. E. *Chem. Eur. J.* **2009**, *15*, 11346–11360. (b) Doster, M. E.; Hatnean, J. A.; Jeftic, T.; Modi, S.; Johnson, S. A. *J. Am. Chem. Soc.* **2010**, *132*, 11923–11925.

(4)   For general aspects of amidate complexes and PYAs, see: (a) Bossu, F. P.; Chellappa, K. L.; Margerum, D. W. *J. Am. Chem. Soc.* **1977**, *99*, 2195–2203. (b) Brzezinski, B.; Zundel, G. *J. Phys. Chem.* **1979**, *83*, 1787–1789. (c) Chien, C.-H.; Leung, M.-K.; Su, J.-K.; Li, G.-H.; Liu, Y.-H.; Wang, Y. *J. Org. Chem.* **2004**, *69*, 1866–1871. (d) Rais, D.; Gould, I. R.; Vilar, R.; White, A. J. P.; Williams, D. J. *Eur. J. Inorg. Chem.* **2004**, 1865–1872. For examples of biological application, see: (e) Li, R.; Martin, M. P.; Liu, Y.; Wang, B.; Patel, R. A.; Zhu, J.-Y.; Sun, N.; Pireddu, R.; Lawrence, N. J.; Li, J.; Haura, E. B.; Sung, S.-S.; Guida, W. C.; Schonbrunn, E.; Sebti, S. M. *J. Med. Chem.*

2012, *55,* 2474–2478. (f) Mishra, A.; Kaushik, N. K.; Verma, A. K.; Gupta, R. *Eur. J. Med. Chem.* **2008**, *43*, 2189–2196.

(5) Boyd, P. D. W.; Wright, L. J.; Zafar, M. N. *Inorg. Chem.* **2011**, *50*, 10522–10524.

(6) Slattery, J.; Thatcher, R. J.; Shi, Q.; Douthwaite, R. E. *Pure Appl. Chem.* **2010**, *82*, 1663–1671.

(7) For examples, see: (a) Fortman, G. C.; Nolan, S. P. *Chem. Soc. Rev.* **2011**, *40*, 5151–5169. (b) Corberan, R.; Mas-Marza, E.; Peris, E. *Eur. J. Inorg. Chem.* **2009**, 1700–1716. (c) Peris, E.; Crabtree, R. H. *Coord. Chem. Rev.* **2004**, *248*, 2239–2246. (d) Scharper, L.-A.; Hock, S. J.; Herrmann, W. A.; Kuehn, F. E. *Angew. Chem. Int. Ed.* **2013**, *52*, 270–289. (e) Grossmann, A.; Enders, P. *Angew. Chem. Int. Ed.* **2012**, *51*, 314–325. (f) César V.; Bellemin-Laponnaz, S.; Gade, L. H. *Chem. Soc. Rev.* **2004**, *33*, 619–636.

(8) (a) Kantchev. E. A. B.; O'Brien, C. J.; Organ, M. G. *Angew. Chem. Int. Ed.* **2007**, *46*, 2768–2813. (b) John, A.; Ghosh, P. *Dalton Trans.* **2010**, *39*, 7183–7206. (c) Lalrempuia, R.; McDaniel, N. D.; Mueller-Bunz, H.; Bernhard, S.; Albrecht, M. *Angew. Chem. Int. Ed.* **2010**, *49*, 9765–9768. (d) Petronilho, A.; Rahman, M.; Woods, J. A.; Al-Sayyed, H.; Mueller-Bunz, H.; MacElroy, J. M. D.; Bernhard, S.; Albrecht, M. *Dalton Trans.* **2012**, *41*, 13074–13080.

(9) Pugh, D.; Danopoulos, A. A. *Coord. Chem. Rev.* **2007**, *251*, 610–641.

(10) Collins, T. J.; Kostka, K. L.; Uffelman, E. S.; Weinberger, T. L. *Inorg. Chem.* **1991**, *30*, 4204–4210.

(11) Xie, H.; Ng, D.; Savinov, S. N.; Dey, B.; Kwong, P. D.; Wyatt, R.; Smith, A. B.; Hendrickson, W. A. *J. Med. Chem.* **2007**, *50*, 4898–4908.

(12) For alternative synthetic strategies, see: (a) Liao, C.-Y.; Chan, K.-T.; Zeng, J.-Y.; Hu, C.-H.; Tu, C.-Y.; Lee, H. M. *Organometallics* **2007**, *26*, 1692–1702. (b) Samantaray, M. K.; Pang, K.; Shaikh, M. M.; Ghosh, P. *Inorg. Chem.* **2008**, *47*, 4153–4165. (c) Unger, Y.; Strassner, T. *J. Organomet. Chem.* **2012**, *713*, 203–208.

(13) Baraldi, P. G.; Preti, D.; Tabrizi, M. A.; Fruttarolo, F.; Saponaro, G.; Baraldi, S.; Romagnoli, R.; Moorman, A. R.; Gessi, S.; Varani, K.; Borea, P. A. *Bioorg. Med. Chem.* **2007**, *15*, 2514–2527.

(14) Huang, S.; Wong, J. C. S.; Leung, A. K. C.; Chan, Y. M.; Wong, L.; Fernendez, M. R.; Miller, A. K.; Wu, W. *Tetrahedron Lett.* **2009**, *50*, 5018–5020.

(15) Sigel, H.; Martin, R. B. *Chem. Rev.* **1982**, *82*, 385–426.

(16) (a) Magil, A. M.; Cavell, K. J.; Yates, B. F. *J. Am. Chem. Soc.* **2004**, *126*, 8717–8724. (b) Massey, R. S.; Collett, C. J.; Lindsay, A. G.; Smith, A. D.; O'Donoghue, A. C. *J. Am. Chem. Soc.* **2012**, *134*, 20421–20432.

(17) (a) Moret, M.-E.; Chaplin, A. B.; Lawrence, A. K.; Scopelliti, R.; Dyson, P. J. *Organometallics* **2005**, *24*, 4039–4048. (b) Horn, S.; Gandolfi, C.; Albrecht, M. *Eur. J. Inorg. Chem.* **2011**, 2863–2868. (c) Gandolfi, C.; Heckenroth, M.; Neels, A.; Laurenczy, C.; Albrecht, M. *Organometallics* **2009**, *28*, 5112–5121. (d) Kaufhold, O.; Flores-Figueroa A.; Pape, T.; Hahn, F. E. *Organometallics* **2009**, *28*, 896–901. (e) Flores-Figueroa A.; Kaufhold, O.; Hepp, A.; Fröhlich, R.; Hahn, F. E. *Organometallics* **2009**, *28*, 6362–6369.

(18) Abbotto, A.; Bradamante, S.; Pagani, G. A. *J. Org. Chem.* **2001**, *66*, 8883–8892.

(19) (a) Cariou, R.; Fischmeister, C.; Toupet, L.; Dixneuf, P. H. *Organometallics* **2006**, *25*, 2126–2128. (b) Clavier, H.; Urbina-Blanco, C. A.; Nolan, S. P. *Organometallics* **2009**, *28*, 2848–2854. (c) Ghattas, W.; Mueller-Bunz, H.; Albrecht, M. *Organometallics* **2010**, *29*, 6782–6789. (d) Bernet, L.; Lalrempuia, R.; Ghattas, W.; Mueller-Bunz, H.; Vigara, L.; Llobet, A.; Albrecht, M. *Chem. Commun.* **2011**, *47*, 8058–8060.

(20) (a) Stander-Grobler, E.; Schuster, O.; Heydenrych, G.; Cronje, S.; Tosh, E.; Albrecht, M.; Frenking, G.; Raubenheimer, H. G. *Organometallics* **2010**, *29*, 5821–5833. (b) Cave, G. W. V.; Hallett, A. J.; Errington, W.; Rourke, J. P. *Angew. Chem. Int. Ed.* **1998**, *37*, 3270–3272. (c) Meguro, H.; Koizumi, T.; Yamamoto, T.; Kanbara, T. *J. Organomet. Chem.* **2008**, *693*, 1109–1106.

(21) However, work in the laboratories of one of us on a related system with an exocyclic C=C bond instead of a C–amide linker as in **3** shows clear double bond localization, yet the corresponding C-N-centroid angle is still large (176.4°), indicating that likely nitrogen does not pyramidalize. Hence this angle may only be a poor probe to distinguish resonance structures **A** and **B**.

(22) Connelly, N. G.; Geiger, W. E. *Chem. Rev.* **1996**, *96*, 877–910.

(23) Leigh, V.; Ghattas, W.; Lalrempuia, R.; Mueller-Bunz, H.; Pryce, M. T.; Albrecht, M. *Inorg. Chem.* **2013**, *52*, 5395–5402.

(24) For a detailed UV-vis spectroscopic study of a pyridinium amide, see: Traore, H.; Saunders, M.; Blasiman, *Aust. J. Chem.* **2000**, *53*, 951–957.

(25) (a) Prades, A.; Viciano, M.; Sanau, M.; Peris, E. *Organometallics* **2008**, *27*, 4254–4259. (b) Marella, R. K.; Neeli, C. K. P.; Kamaraju, S. R. R.; Burri, D. R. *Catal. Sci. Technol.* **2012**, *2*, 1833–838. (c) Davies, R. R.; Hodgson, H. H. *J. Chem. Soc.* **1943**, 282–284.

(26) Griffiths, T. R.; Pugh, D. C. *Coord. Chem. Rev.* **1979**, *29* 129–211.

(27) Canseco-Gonzales, D.; Albrecht, M. *Dalton Trans.* **2013**, *42*, 7424–7432.

(28) Starikova, O. V.; Dolgushin, G. V.; Larina, L. I.; Ushakov, P. E.; Komarova, T. N.; Lopyrev, V. A. *Russ. J. Org. Chem.* **2003**, *39*, 1467–1470.

(29) Clark, R. C.; Reid, J. S. *Acta Cryst.* **1995**, *A51*, 887–897.

(30) Sheldrick, G. M. *Acta Cryst.* **2008**, *A64*, 112–122.

(31) Spek, A. L. *J. Appl. Cryst.* **2003**, *36*, 7–13.

For Tables of Content Only
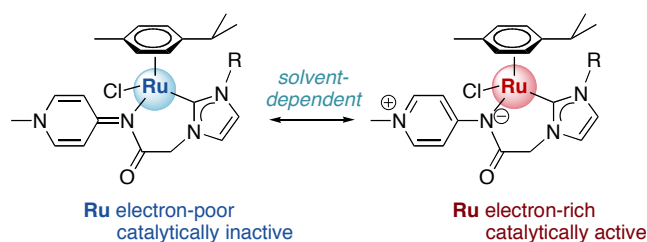
A chelating hybrid ligand containing a pyridinylidene amide (PYA) and a N-heterocyclic carbene donor site adapts its donor ability in response to the solvent medium, comprising either a π-acidic imine neutral resonance form or a strongly σ-donating mesoionic resonance form of the PYA unit. These differences in donor ability have direct implications for redox and catalytic applications.